

On the Performance of Multicarrier DS-CDMA With Imperfect Power Control and Variable Spreading Factors

Li-Chun Wang, *Senior Member, IEEE*, and Chih-Wen Chang, *Student Member, IEEE*

Abstract—Multicarrier direct-sequence code-division multiple access (MC-DS-CDMA) becomes an attractive technique for the future fourth-generation (4G) wireless system because it can flexibly adapt transmission rates by changing both time and frequency spreading factors and possesses many physical-layer advantages in dispersive fading channels. However, power control errors (PCE) and the complete multiple access interference (MAI) from all the intersubcarriers may significantly degrade the performance of the MC-DS-CDMA system. In this paper, we propose an analytical method to evaluate the joint effects of the PCE and the complete MAI on the multirate MC-DS-CDMA system. From analysis and simulation, we obtain some important insights into the performance issues of the MC-DS-CDMA system. First, the effect of PCE can exacerbate the impact of the complete MAI on the MC-DS-CDMA system, or *vice versa*. For $\text{BER} = 10^{-3}$ in a considered case, the joint effect of the complete MAI and PCE further degrades the performance by 2.1 dB compared with the sum of the degradation from the complete MAI and the PCE individually. Second, increasing frequency- or time-domain spreading gain can improve the performance of the MC-DS-CDMA system, but the system also becomes more sensitive to power control errors. Third, a larger PCE can possibly make the frequency-domain diversity diminish faster than the gain obtained from the time-domain spreading although an MC-DS-CDMA system with a larger frequency-domain spreading gain (M) is usually better than that with a larger time-domain spreading gain (G_o). In our example, for the standard deviation of PCE (σ_e) equal to 0 dB, the BERs with $(M, G_o) = (4, 16)$ and $(16, 4)$ are 9.3×10^{-4} and 3.7×10^{-5} , respectively, while for $\sigma_e = 4$ dB, the BER performances of the two cases are all in the order of 10^{-3} .

Index Terms—Multicarrier direct-sequence code-division multiple access (MC-DS-CDMA), power control, power control errors.

I. INTRODUCTION

MULTICARRIER direct-sequence code-division multiple access (MC-DS-CDMA), a combination of multicarrier modulation and spread-spectrum, has become an important technique for the fourth-generation (4G) wireless systems [1]–[4]. The advantages of the MC-DS-CDMA system include the immunity to the dispersive fading channel, less peak-to-average power ratio compared with the orthogonal frequency-

division multiplexing (OFDM) system, and the flexibility of assigning spreading factors in both the frequency and time domains. Pure frequency spreading, pure time spreading, and joint time and frequency spreading are three spreading methods for the MC-DS-CDMA systems. It has been reported that MC-DS-CDMA using both time and frequency spreading codes outperforms the pure time or frequency spreading methods [5].

Although MC-DS-CDMA has been extensively studied recently [6]–[10], to our knowledge, the effects of power control errors (PCE) on MC-DS-CDMA seem to be neglected. Improper power control may significantly degrade the performance of the MC-DS-CDMA system. The key question is how to quantitatively analyze the impact of power control errors on the MC-DS-CDMA system. Unlike most current papers in the subject of MC-DS-CDMA assuming perfect power control, the first goal of this paper is to investigate the impact of open-loop power control errors on the MC-DS-CDMA systems. In general, power control schemes can be divided into two categories: the closed-loop power control and the open-loop power control. The former technique is to combat the small scale fading such as the Rayleigh-fading caused by multipath propagation, while the latter one aims to resolve the near-far effect, owing to the large-scale fading caused by path loss and shadowing, in a multiuser CDMA system. Note that with open-loop power control to overcome the near-far effect, each subcarrier may still experience severe multipath fast fading.

The second objective of this paper is to analyze the effect of the *complete* multiple access interference (MAI) on top of power control errors for the *multirate* MC-DS-CDMA system. To support various types of services in the 4G system, MC-DS-CDMA becomes an attractive technique because it can adapt transmission rates by dynamically changing time and frequency spreading factors. However, most analytical models for the MC-DS-CDMA system are mainly focused on the single rate case. In a multirate MC-DS-CDMA system, the MAI issue becomes more involved because the users with different transmission rates may cause different levels of the MAI. In addition, asynchronous transmissions among users is another critical performance issue. Asynchronous users may destroy the orthogonality between subcarriers in the MC-DS-CDMA system. To our knowledge, the effect of the complete MAI (i.e., the interference from the main subcarrier and all the adjacent subcarriers of other users) has not yet been fully investigated in the context of the multirate MC-DS-CDMA system. Hence,

Manuscript received April 1, 2005; revised October 1, 2005. This work was supported in part by the National Science Council and in part the Program of Promoting University Excellence of Ministry of Education, Taiwan under Contract 93-2219-E-009-012 and Contract EX-91-E-FA06-4-4. This paper was presented in part at the 2005 IEEE Global Telecommunications Conference, St. Louis, MI, November 28–December 2, 2005.

The authors are with the Department of Communication Engineering, National Chiao Tung University, Hsinchu 300, Taiwan, R.O.C. (e-mail: lichun@cc.nctu.edu.tw; cwchang.tw@gmail.com).

Digital Object Identifier 10.1109/JSAC.2005.864025

we are motivated to develop an analytical model to evaluate the effects of the complete MAI of asynchronous multirate users for the MC-DS-CDMA system.

In the literature, the studies on the performance of the MC-DS-CDMA system subject to power control errors and MAI can be summarized twofold. On the one hand, from the standpoint of MAI, the authors in [11] analyzed the MAI's effect from the main subcarrier for a single-rate MC-DS-CDMA system. In [12], the authors analyzed the effect of the other intersubcarriers' MAI in the MC-DS-CDMA system, but only for the single-rate case. The authors in [13] analyzed the performance of the multirate multicarrier DS-CDMA systems, but considered only the effect of the MAI from the main subcarrier. On the other hand, from the view point of power control errors, most studies for the MC-DS-CDMA systems were performed with the assumption of perfect power control [11]–[13]. Although power control has been extensively studied for the single-carrier DS-CDMA system in the literature [14]–[18], extending these results from the single-carrier case to the multicarrier case is a nontrivial task because the effect of power control errors in an MC-DS-CDMA system has to be jointly evaluated with the complete MAI from all intersubcarriers.

In summary, in this paper, we develop an analytical model to characterize the joint effects of both the PCE and the complete MAI for the multirate MC-DS-CDMA system. Applying the developed analytical model, we obtain some important insights into the performance issues of the MC-DS-CDMA system. First, when both PCE and the complete MAI are jointly considered, the effect of PCE can exacerbate the impact of complete MAI on MC-DS-CDMA, or *vice versa*. That is, the joint impact of complete MAI and PCE is actually severer than the summation of the performance degradation from the complete MAI and PCE individually. Second, increasing the maximum total spreading gain by either increasing frequency- or time-domain spreading gain can enhance the error rate performance for the multirate MC-DS-CDMA system, but it is necessary to pay attention to the side effect of higher sensitivity to power control errors. Third, for the same total time and frequency spreading gain, an MC-DS-CDMA system with a larger frequency-domain spreading factor outperforms the system with a larger time-domain spreading factor. However, the performance differences between the two are shrunk as power control errors increase.

The rest of this paper is organized as follows. In Section II, we introduce the signal and system models of the MC-DS-CDMA system using both time- and frequency-domain spreading codes. In Section III, we derive the error rate probability for the multirate MC-DS-CDMA system taking into account of the complete MAI. In Section IV, we discuss the impact of PCE on the multi-

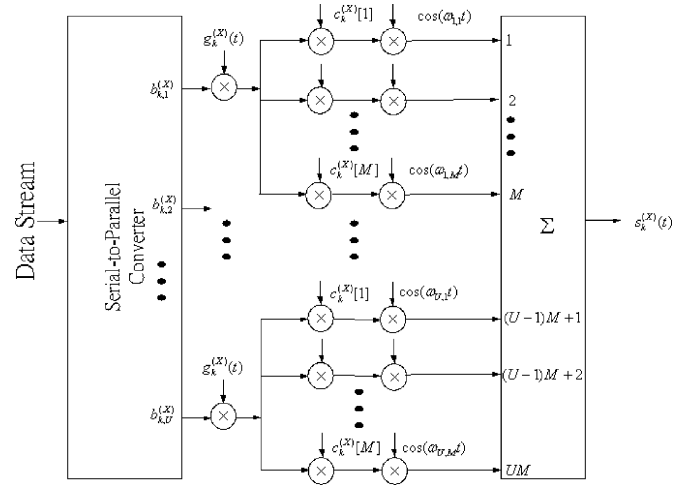


Fig. 1. The transmitter structure of the MC-DS-CDMA system using time- and frequency-domain spreading codes.

rate MC-DS-CDMA system. Numerical results are provided in Section V. Section VI gives concluding remarks.

II. SYSTEM MODEL

A. Transmitted Signal

The transmitter structure in the MC-DS-CDMA system using both time- and frequency-domain spreading codes is shown in Fig. 1. First, the serial-to-parallel process converts a data stream with the duration of $T_{b,k}^{(X)}$ to U slower parallel with bit duration $T_k^{(X)} = UT_{b,k}^{(X)}$, where k is the user index and the user group $X \in A, B, C$ will be defined later. After the serial-to-parallel processing, unlike that the original data stream is transmitted in a frequency-selective fading channel, each substream is now transmitted in a frequency flat (or nondispersive) fading channel. In the next step, the data in each substream are spread by a time-domain spreading code $g_k^{(X)}(t)$. Being copied to M subcarriers, each substream is multiplied by a frequency-domain spreading code $\{c_k^{(X)}[j]\}$.

The transmitted signal of user k in group X can be expressed in (1) shown at the bottom of the page, where $P_k^{(X)}$ and $\lambda_k^{(X)}$, respectively, represent the transmitted power and the PCE, while $\{f_{i,j}\}$ and $\{\varphi_{k,i,j}\}$ represent the subcarrier frequency and the initial phase for the j th carrier of the i th substream, respectively. The waveform in the i th substream $b_{k,i}^{(X)}(t) = \sum_{h=-\infty}^{\infty} b_{k,i}^{(X)}[h]P_{T_k^{(X)}}(t - hT_k^{(X)})$ consists of a sequence of independent rectangular pulses with duration $T_k^{(X)}$, where $b_{k,i}^{(X)}[h] = \pm 1$ with equal probability. The time-domain spreading code $g_k^{(X)}(t) = \sum_{\ell=-\infty}^{\infty} g_k^{(X)}[\ell]P_{T_c}(t - \ell T_c)$ rep-

$$s_k^{(X)}(t) = \sum_{i=1}^U \sum_{j=1}^M \sqrt{\frac{2\lambda_k^{(X)} P_k^{(X)}}{M}} b_{k,i}^{(X)}(t) g_k^{(X)}(t) c_k^{(X)}[j] \cos(2\pi f_{i,j} t + \varphi_{k,i,j}^{(X)}) \quad (1)$$

resents the chip sequence of the rectangular pulses of duration T_c , where $g_k^{(\mathbf{X})}[\ell] = \pm 1$ with equal probability. Note that the time-domain spreading factor of user k in the group \mathbf{X} is $G_k^{(\mathbf{X})} = T_k^{(\mathbf{X})}/T_c$.

The user group \mathbf{X} is defined as follows. Let $g_o(t)$ and $c_o[j]$ be the time-domain spreading code and frequency-domain spreading code of the reference user, respectively. As in [11], we categorize the interfering users into three groups.

- 1) **Group A:** the user utilizing a time-domain spreading code $g_k^{(\mathbf{A})}(t) = g_o(t)$ and a frequency-domain spreading code $c_k^{(\mathbf{A})}[j] \neq c_o[j]$.
- 2) **Group B:** the user utilizing a time-domain spreading code $g_k^{(\mathbf{B})}(t) \neq g_o(t)$ and a frequency-domain spreading code $c_k^{(\mathbf{B})}[j] = c_o[j]$.
- 3) **Group C:** the user utilizing a time-domain spreading code $g_k^{(\mathbf{C})}(t) \neq g_o(t)$ and a frequency-domain spreading code $c_k^{(\mathbf{C})}[j] \neq c_o[j]$.

Noteworthy, $g_k^{(\mathbf{X})}(t) \neq g_o(t)$ (or $c_k^{(\mathbf{X})}[j] \neq c_o[j]$) can also be the case with the same particular pseudonoise sequence offset by two different values.

B. Received Signal

Since each substream is sent in the flat Rayleigh-fading channel, the received signal of the reference user (denoted by r_o), can be expressed in (2) shown at the bottom of the page, where P_o and λ_o , respectively, represent the transmitted power and the PCE of the reference user; $\alpha_{o,i,j}$ and $\alpha_{k,i,j}^{(\mathbf{X})}$ are the channel's amplitude of the reference user and that of the k th user in group \mathbf{X} , respectively; τ_o is the propagation delay for the reference user which is assumed to be $\tau_o = 0$ without loss of generality; $\tau_k^{(\mathbf{X})}$ is the misalignment with respect to the reference user, which is uniformly distributed in the time interval $[0, T_k^{(\mathbf{X})}]$; $K_{\mathbf{X}}$ is the number of users in the group \mathbf{X} ; and $n(t)$ is the white Gaussian noise with double-sided power spectrum density of $N_0/2$. In (2), $\phi_{o,i,j} = \varphi_{o,i,j} + \psi_{o,i,j} - 2\pi f_{i,j}\tau_o$ and $\phi_{k,i,j}^{(\mathbf{X})} = \varphi_{k,i,j}^{(\mathbf{X})} + \psi_{k,i,j}^{(\mathbf{X})} - 2\pi f_{i,j}\tau_k^{(\mathbf{X})}$ are uniformly distributed in $[0, 2\pi)$, where $\varphi_{o,i,j}$ and $\psi_{o,i,j}$ are the initial phase and the channel's phase of the reference user, and $\varphi_{k,i,j}^{(\mathbf{X})}$ and $\psi_{k,i,j}^{(\mathbf{X})}$ are those for the k th user in group \mathbf{X} , respectively.

The receiver structure of the MC-DS-CDMA system using time-domain and frequency-domain spreading codes is shown in Fig. 2. Without loss of generality, let the bit of interest be the first bit in the s th substream of the reference user (denoted by $b_{o,s}[0]$). After time-domain despreading, the output variable in

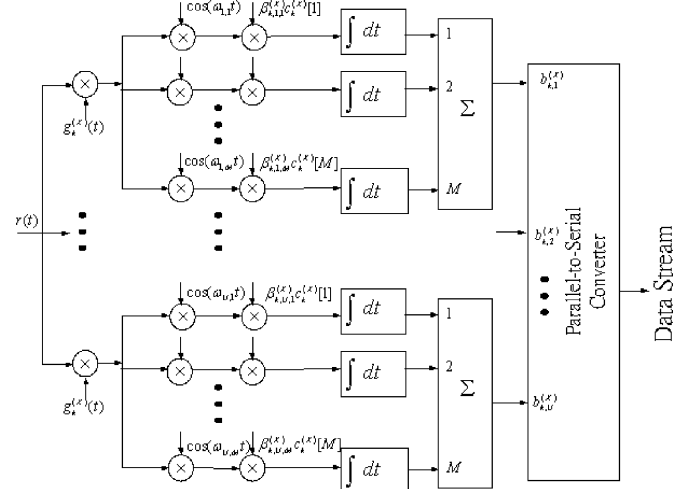


Fig. 2. The receiver structure of the MC-DS-CDMA system using time- and frequency-domain spreading codes.

the v th subcarrier of the s th substream for the reference user can be expressed as

$$\begin{aligned}
 Y_{o,s,v} &= \int_0^{T_o} r_o(t) \beta_{o,s,v} g_o(t) c_o[v] \cos(2\pi f_{s,v}t + \phi_{o,s,v}) dt \\
 &= \sqrt{\frac{\lambda_o P_o}{2M}} T_o \left\{ b_{o,s}[0] \alpha_{o,s,v} \beta_{o,s,v} \right. \\
 &\quad \left. + \sum_{\mathbf{X} \in \{\mathbf{A}, \mathbf{B}, \mathbf{C}\}} \left[\sum_{k=1}^{K_{\mathbf{X}}} I_{\mathbf{X},k}^{(1)} + \sum_{k=1}^{K_{\mathbf{X}}} \underbrace{\sum_{i=1}^U \sum_{j=1}^M}_{j \neq v \text{ for } i=s} I_{\mathbf{X},k}^{(2)} \right] + n_{s,v} \right\} \quad (3)
 \end{aligned}$$

where P_o and T_o are the transmit power and the bit duration of the reference user; $\beta_{o,s,v}$ is the weights for a certain combining scheme; $I_{\mathbf{X},k}^{(1)}$ and $I_{\mathbf{X},k}^{(2)}$ denote the MAI from the main subcarrier and that from other intersubcarriers, respectively; and $n_{s,v}$ is the white Gaussian noise with zero mean and variance of $(|\beta_{o,s,v}|^2/2\lambda_o)(E_o/MN_0)^{-1}$, where $E_o = P_o T_o$ is the bit energy of the reference user. Combining M subcarriers, the decision variable of $b_{o,s}[0]$ for the reference user becomes

$$Y_{o,s} = \sum_{v=1}^M Y_{o,s,v} \quad (4)$$

where $Y_{o,s,v}$ is given in (3).

$$\begin{aligned}
 r_o(t) &= \sum_{i=1}^U \sum_{j=1}^M \sqrt{\frac{2\lambda_o P_o}{M}} \alpha_{o,i,j} b_{o,i}(t - \tau_o) g_o(t - \tau_o) c_o[j] \cos(2\pi f_{i,j}t + \phi_{o,i,j}) \\
 &\quad + \sum_{\mathbf{X} \in \{\mathbf{A}, \mathbf{B}, \mathbf{C}\}} \sum_{k=1}^{K_{\mathbf{X}}} \sum_{i=1}^U \sum_{j=1}^M \sqrt{\frac{2\lambda_k^{(\mathbf{X})} P_k^{(\mathbf{X})}}{M}} \alpha_{k,i,j}^{(\mathbf{X})} b_{k,i}^{(\mathbf{X})}(t - \tau_k^{(\mathbf{X})}) \times g_k^{(\mathbf{X})}(t - \tau_k^{(\mathbf{X})}) c_k^{(\mathbf{X})}[j] \cos(2\pi f_{i,j}t + \phi_{k,i,j}^{(\mathbf{X})}) + n(t) \quad (2)
 \end{aligned}$$

C. Assumption

To make $Y_{o,s}$ have the maximal diversity combining gain, we assume that the associated M subcarriers in (4) experience independent fading. For this purpose, any two neighboring subcarriers in the same substream are at least separated by the maximal coherent bandwidth, denoted by $\max(BW_c)$. Denote Δ_f the minimal frequency spacing between any two adjacent substreams with the same subcarrier index. Then, $f_{i,j}$ (the frequency of the j th subcarrier of the i th substream) can be determined by the following rule:

$$f_{i,j} = f_o + [(i-1) + (j-1)U]\Delta_f, \text{ for } \begin{cases} 1 \leq i \leq U \\ 1 \leq j \leq M \end{cases} \quad (5)$$

where f_o is the main carrier frequency. In order to achieve the maximum diversity combining gain in (4), the following condition:

$$U\Delta_f \geq \max(BW_c) \quad (6)$$

should be satisfied, where U is the size of the serial-to-parallel process. Note that the system bandwidth is proportional to UMG_o/T_o . For a fixed total number of subcarriers (UM), U should be large enough to satisfy the condition of (6). Otherwise, the assumption of independent subcarriers may become less realistic.

III. EFFECT OF COMPLETE MAI ON BIT-ERROR RATE (BER) PERFORMANCE

A. Motivation

The complete MAI in a multirate MC-DS-CDMA system is defined as the sum of the other users's interference form their main subcarrier and all the other intersubcarriers. For any two synchronous transmissions at subcarriers $f_{s,v}$ and $f_{i,j}$ with the initial phase $\phi_{s,v}$ and $\phi_{i,j}$, respectively, the orthogonality requirement

$$\int_0^{T_c} \cos(2\pi f_{s,v}t + \phi_{s,v})\cos(2\pi f_{i,j}t + \phi_{i,j})dt = 0 \quad (7)$$

can be fulfilled if the following condition is sustained:

$$|f_{s,v} - f_{i,j}| = \frac{h}{T_c} \quad (8)$$

where h is nonzero positive integer and T_c is the chip duration.

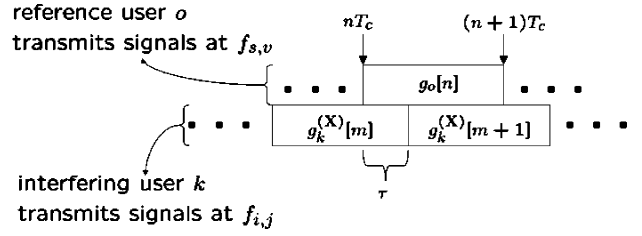


Fig. 3. An illustrative example of intersubcarrier interference for asynchronous users, where the misalignment between the reference user o and the interfering user k in group \mathbf{X} by τ .

However, for asynchronous users, the orthogonality condition between subcarriers can not be held anymore. Assume that the reference user and the interfering user k in group \mathbf{X} is misaligned by τ , where $0 < \tau < T_c$. As shown in Fig. 3, we consider the $(n+1)$ th chip of the reference user, during which the interfering user sends part of the $(m+1)$ th chip and part of the $(m+2)$ th chip. Recall that $g_o[n]$ denotes the $(n+1)$ th chip of the spreading code of the reference user and $g_k^{(X)}[m]$ denotes the $(m+1)$ th chip of the spreading code of the interfering user. Suppose that the reference and the interfering users transmit data at subcarriers $f_{s,v}$ and $f_{i,j}$, respectively, and define the unit step function $H(t)$ as

$$H(t) = \begin{cases} 1, & t \geq 0 \\ 0, & t < 0 \end{cases} \quad (9)$$

We can express the cross correlation between the two subcarriers $f_{s,v}$ and $f_{i,j}$ during the $(n+1)$ th chip as shown in (10) at the bottom of the page, where ξ is a nonzero value. Clearly, the orthogonality between subcarriers of the two users can no longer be ensured for asynchronously transmitted data. Thus, in addition to the MAI from the main subcarrier in an MC-DS-CDMA system, it is also important to evaluate this kind of other intersubcarriers' MAI.

B. BER Performance

We denote the MAI from the main subcarrier by $I_{\mathbf{X},k}^{(1)}$ and the MAI from other intersubcarriers, by $I_{\mathbf{X},k}^{(2)}$, respectively. As in [7] and [12], both types of MAIs are modeled by a zero-mean Gaussian random variable. Because $I_{\mathbf{X},k}^{(1)}$ can be obtained from $I_{\mathbf{X},k}^{(2)}$ by letting $f_{i,j} = f_{s,v}$, we first analyze $I_{\mathbf{X},k}^{(2)}$. To analyze the MAI in the case of multirate transmissions, we further consider two scenarios according to the relationship between T_o (the bit

$$\begin{aligned} & \int_{nT_c}^{(n+1)T_c} g_o[n]\cos(2\pi f_{s,v}t + \phi_{s,v}) \left[g_k^{(X)}[m][H(nT_c) - H(nT_c + \tau)] \right. \\ & \quad \left. + g_k^{(X)}[m+1][H(nT_c + \tau) - H((n+1)T_c)] \right] \cos(2\pi f_{i,j}(t - \tau) + \phi_{i,j})dt \\ & = g_o[n]g_k^{(X)}[m] \int_{nT_c}^{nT_c + \tau} \cos(2\pi f_{s,v}t + \phi_{s,v})\cos(2\pi f_{i,j}t + \phi_{i,j} - 2\pi f_{i,j}\tau)dt \\ & \quad + g_o[n]g_k^{(X)}[m+1] \times \int_{nT_c + \tau}^{(n+1)T_c} \cos(2\pi f_{s,v}t + \phi_{s,v})\cos(2\pi f_{i,j}t + \phi_{i,j} - 2\pi f_{i,j}\tau)dt \\ & = \begin{cases} \xi \neq 0, & \text{when } g_o[n]g_k^{(X)}[m] \neq g_o[n]g_k^{(X)}[m+1] \\ 0, & \text{otherwise} \end{cases} \quad (10) \end{aligned}$$

duration of the reference user) and $T_k^{(\mathbf{X})}$ (bit duration of the interfering user).

1) *Other Intersubcarriers' MAI From Low Data Rate Users:* In this case $T_o \leq T_k^{(\mathbf{X})}$. Since $\tau_k^{(\mathbf{X})}$ is uniformly distributed in the interval $[0, T_k^{(\mathbf{X})})$, $\tau_k^{(\mathbf{X})}$ may fall into two possible regions: a) $0 \leq \tau_k^{(\mathbf{X})} < T_o$ and b) $T_o \leq \tau_k^{(\mathbf{X})} < T_k^{(\mathbf{X})}$. Clearly, the probability of $\tau_k^{(\mathbf{X})}$ falling in region a) is

$$P(0 \leq \tau_k^{(\mathbf{X})} < T_o) = \frac{T_o}{T_k^{(\mathbf{X})}} \quad (11)$$

and that of $\tau_k^{(\mathbf{X})}$ falling in region b) is

$$P(T_o \leq \tau_k^{(\mathbf{X})} < T_k^{(\mathbf{X})}) = \frac{T_k^{(\mathbf{X})} - T_o}{T_k^{(\mathbf{X})}}. \quad (12)$$

Denote $I_{\mathbf{X},k}^{(2)'}$ and $I_{\mathbf{X},k}^{(2)''}$ the MAI from other intersubcarriers in cases a) and b), respectively. Let $b_{o,s}[0]$ be the bit of interest. Referring to (3) and (10), the MAI from the j th subcarrier of the i th substream ($f_{i,j}$) to the desired v th subcarrier of the s th substream ($f_{s,v}$) can be expressed in (13) shown at the bottom of the page, where $\theta_{k,i,j}^{(\mathbf{X})} = \phi_{k,i,j} - \phi_{o,s,v}$ is uniformly distributed in $[0, 2\pi)$

$$\begin{aligned} & R(\tau_k^{(\mathbf{X})}, \theta_{k,i,j}^{(\mathbf{X})}) \\ &= \int_0^{\tau_k^{(\mathbf{X})}} g_k^{(\mathbf{X})}(t - \tau_k^{(\mathbf{X})}) g_o(t) \cos(2\pi(f_{i,j} - f_{s,v})t + \theta_{k,i,j}^{(\mathbf{X})}) dt; \end{aligned} \quad (14)$$

$$\begin{aligned} & \tilde{R}(\tau_k^{(\mathbf{X})}, \theta_{k,i,j}^{(\mathbf{X})}) \\ &= \int_{\tau_k^{(\mathbf{X})}}^{T_o} g_k^{(\mathbf{X})}(t - \tau_k^{(\mathbf{X})}) g_o(t) \cos(2\pi(f_{i,j} - f_{s,v})t + \theta_{k,i,j}^{(\mathbf{X})}) dt. \end{aligned} \quad (15)$$

Similarly, we can express $I_{\mathbf{X},k}^{(2)''}$ as

$$\begin{aligned} I_{\mathbf{X},k}^{(2)''} &= \sqrt{\frac{\lambda_k^{(\mathbf{X})} P_k^{(\mathbf{X})}}{\lambda_o P_o} \frac{\alpha_{k,i,j}^{(\mathbf{X})} \beta_{o,s,v} c_k^{(\mathbf{X})}[j] c_o[v]}{T_o}} \left[b_{k,i}^{(\mathbf{X})}[-1] \right. \\ & \quad \left. \times R(T_o, \theta_{k,i,j}^{(\mathbf{X})}) \right] \end{aligned} \quad (16)$$

where

$$\begin{aligned} & R(T_o, \theta_{k,i,j}^{(\mathbf{X})}) \\ &= \int_0^{T_o} g_k^{(\mathbf{X})}(t - \tau_k^{(\mathbf{X})}) g_o(t) \times \cos(2\pi(f_{i,j} - f_{s,v})t + \theta_{k,i,j}^{(\mathbf{X})}) dt. \end{aligned} \quad (17)$$

Note that (16) only exists for the multirate transmissions, which is not seen in the single rate case. Because it is assumed that

the MAI can be approximated by a Gaussian distributed random variable, we express the variance of $I_{\mathbf{X},k}^{(2)'}$ and $I_{\mathbf{X},k}^{(2)''}$ as follows:

$$\begin{aligned} \text{Var}[I_{\mathbf{X},k}^{(2)'}] &= \frac{\bar{\lambda} P_k^{(\mathbf{X})}}{\lambda_o P_o} \frac{E[(\alpha_{k,i,j}^{(\mathbf{X})})^2] \beta_{o,s,v}^2}{T_o^2} \{ \text{Var}[R(\tau_k^{(\mathbf{X})}, \theta_{k,i,j}^{(\mathbf{X})})] \\ & \quad + \text{Var}[\tilde{R}(\tau_k^{(\mathbf{X})}, \theta_{k,i,j}^{(\mathbf{X})})] \} \end{aligned} \quad (18)$$

and

$$\text{Var}[I_{\mathbf{X},k}^{(2)''}] = \frac{\bar{\lambda} P_k^{(\mathbf{X})}}{\lambda_o P_o} \frac{E[(\alpha_{k,i,j}^{(\mathbf{X})})^2] \beta_{o,s,v}^2}{T_o^2} \{ \text{Var}[R(T_o, \theta_{k,i,j}^{(\mathbf{X})})] \}. \quad (19)$$

The detail derivations of $R(\tau_k^{(\mathbf{X})}, \theta_{k,i,j}^{(\mathbf{X})})$, $\tilde{R}(\tau_k^{(\mathbf{X})}, \theta_{k,i,j}^{(\mathbf{X})})$, and $R(T_o, \theta_{k,i,j}^{(\mathbf{X})})$ can be found in Appendices A and B. Note that $E[(\alpha_{k,i,j}^{(\mathbf{X})})^2] = 1$ for the flat Rayleigh-fading channel. The distributions of power control errors among all the users are assumed to be the same. Denote $\bar{\lambda} = E[\lambda_k^{(\mathbf{X})}]$ the average power control error. After some derivations, we can have

$$\begin{aligned} \text{Var}[I_{\mathbf{X},k}^{(2)'}] &= \text{Var}[I_{\mathbf{X},k}^{(2)''}] \\ &= \frac{\bar{\lambda} P_k^{(\mathbf{X})}}{\lambda_o P_o} \frac{\beta_{o,s,v}^2}{2G_o \pi^2 [(i-s) + (j-v)U]^2}. \end{aligned} \quad (20)$$

From (11), (12), (19), and (20), it is followed that:

$$\begin{aligned} \text{Var}[I_{\mathbf{X},k}^{(2)}] &= \text{Var}[I_{\mathbf{X},k}^{(2)'}] P(0 \leq \tau_k^{(\mathbf{X})} < T_o) \\ & \quad + \text{Var}[I_{\mathbf{X},k}^{(2)''}] P(T_o \leq \tau_k^{(\mathbf{X})} < T_k^{(\mathbf{X})}) \end{aligned} \quad (21)$$

$$= \frac{\bar{\lambda} P_k^{(\mathbf{X})}}{\lambda_o P_o} \frac{\beta_{o,s,v}^2}{2G_o \pi^2 [(i-s) + (j-v)U]^2}. \quad (22)$$

2) *Other Intersubcarriers' MAI From High Data Rate Users:* In this case, $T_o > T_k^{(\mathbf{X})}$. Assume $T_o = LT_k^{(\mathbf{X})}$, where L is a positive integer. Similarly, by referring to (3) and (10), we express the MAI from the j th subcarrier of the i th substream ($f_{i,j}$) to the desired v th subcarrier of the s th substream ($f_{s,v}$) as follows in (23) shown at the bottom of the next page, where (24)–(25) are shown at the bottom of the next page. Note that (23) exists only for the multirate transmissions. Following the procedures of deriving (20), we obtain

$$\text{Var}[I_{\mathbf{X},k}^{(2)}] = \frac{\bar{\lambda} P_k^{(\mathbf{X})}}{\lambda_o P_o} \frac{\beta_{o,s,v}^2}{2G_o \pi^2 [(i-s) + (j-v)U]^2}. \quad (26)$$

3) *Main Subcarriers' MAI:* Let $z = (i-s) + (j-v)U$ in (26). Referring to [12], we can obtain the variance of the main subcarriers' MAI from the low or high data rate users as

$$\text{Var}[I_{\mathbf{X},k}^{(1)}] = \lim_{z \rightarrow 0} \text{Var}[I_{\mathbf{X},k}^{(2)}] = \frac{\bar{\lambda}}{\lambda_o} \frac{P_k^{(\mathbf{X})}}{P_o} \frac{\beta_{o,s,v}^2}{3G_o}. \quad (27)$$

$$\begin{aligned} I_{\mathbf{X},k}^{(2)'} &= \sqrt{\frac{\lambda_k^{(\mathbf{X})} P_k^{(\mathbf{X})}}{\lambda_o P_o} \frac{\alpha_{k,i,j}^{(\mathbf{X})} \beta_{o,s,v} c_k^{(\mathbf{X})}[j] c_o[v]}{T_o}} \\ & \quad \times \int_0^{T_o} b_{k,i}^{(\mathbf{X})}(t - \tau_k^{(\mathbf{X})}) g_k^{(\mathbf{X})}(t - \tau_k^{(\mathbf{X})}) g_o(t) \cos(2\pi(f_{i,j} - f_{s,v})t + \theta_{k,i,j}^{(\mathbf{X})}) dt \\ &= \sqrt{\frac{\lambda_k^{(\mathbf{X})} P_k^{(\mathbf{X})}}{\lambda_o P_o} \frac{\alpha_{k,i,j}^{(\mathbf{X})} \beta_{o,s,v} c_k^{(\mathbf{X})}[j] c_o[v]}{T_o}} \left[b_{k,i}^{(\mathbf{X})}[-1] R(\tau_k^{(\mathbf{X})}, \theta_{k,i,j}^{(\mathbf{X})}) + b_{k,i}^{(\mathbf{X})}[0] \tilde{R}(\tau_k^{(\mathbf{X})}, \theta_{k,i,j}^{(\mathbf{X})}) \right] \end{aligned} \quad (13)$$

Note that in (22), (26), and (27), the effects of multirate transmissions and PCE are included in $P_k^{(\mathbf{X})}/P_o$ and $\bar{\lambda}/\lambda_o$, respectively.

C. The Statistics of the Decision Variable $Y_{o,s}$

Consider the maximum ratio combining scheme and choose the weighting factor $(\beta_{o,s,v})$ as the complex conjugate of the channel response of the reference user $(\alpha_{o,s,v})$. The decision variable $Y_{o,s}$ is also a Gaussian distributed random variable since the MAI is modeled by a Gaussian distributed random variable. Combining (3), (4), (26), and (27) and averaging $Y_{o,s}$ over s and v , we can express the mean and the variance of $Y_{o,s}$ with a frequency-domain spreading factor M as follows:

$$E[Y_{o,s}] = b_{o,s}[0] \sum_{v=1}^M |\alpha_{o,s,v}|^2 \quad (28)$$

and

$$\begin{aligned} \text{Var}[Y_{o,s}] = & \left[\frac{1}{2\lambda_o} \left(\frac{E_o}{MN_0} \right)^{-1} + \sum_{\mathbf{X} \in \{\mathbf{A}, \mathbf{B}, \mathbf{C}\}} \sum_{k=1}^{K_{\mathbf{X}}} \frac{\bar{\lambda}}{\lambda_o} \frac{P_k^{(\mathbf{X})}}{P_o G_o} \right. \\ & \left. \times \left(\frac{1}{3} + (UM-1)I_{oc} \right) \right] \sum_{v=1}^M |\alpha_{o,s,v}|^2 \quad (29) \end{aligned}$$

where

$$\begin{aligned} I_{oc} = & \frac{1}{UM} \\ & \times \sum_{s=1}^U \sum_{v=1}^M \left\{ \frac{1}{UM-1} \times \sum_{\substack{i=1 \\ j \neq v \text{ for } i=s}}^M \left[\frac{1}{2\pi^2 [(i-s) + (j-v)U]^2} \right] \right\}. \quad (30) \end{aligned}$$

Define the received signal to noise ratio (denoted by γ) as

$$\gamma = \frac{E^2[Y_{o,s}]}{2\text{Var}[Y_{o,s}]}. \quad (31)$$

Substituting (28) and (29) into (31), we can have

$$\gamma = \lambda_o \gamma_c \gamma_L \quad (32)$$

where

$$\begin{aligned} \gamma_c = & \left[\left(\frac{E_o}{MN_0} \right)^{-1} \right. \\ & \left. + \sum_{\mathbf{X} \in \{\mathbf{A}, \mathbf{B}, \mathbf{C}\}} \sum_{k=1}^{K_{\mathbf{X}}} \frac{2\bar{\lambda}P_k^{(\mathbf{X})}}{P_o G_o} \times \left(\frac{1}{3} + (UM-1)I_{oc} \right) \right]^{-1} \quad (33) \end{aligned}$$

is a parameter to characterize the joint effects of the complete MAI and power control errors and

$$\gamma_L = \sum_{v=1}^M |\alpha_{o,s,v}|^2 \quad (34)$$

is the central chi-square distributed random variable with $2M$ degrees of freedom. From [19], the probability density function (pdf) of γ_L is given by

$$f(\gamma_L) = \frac{1}{(M-1)!} \gamma_L^{M-1} e^{-\gamma_L}, \quad \text{for } \gamma_L \geq 0. \quad (35)$$

Like [13] and [20], we let $P_k^{(\mathbf{X})}/P_o = R_k^{(\mathbf{X})}/R_o$ in (29) and (33), where R_o and $R_k^{(\mathbf{X})}$ are the transmission rates of the reference user and user k in group \mathbf{X} , respectively. This implies that a user needs more power to support higher transmission rate.

For binary phase-shift keying modulation with coherent detection, the conditional error probability for a given γ_L and λ_o is equal to

$$P(e|\gamma_L, \lambda_o) = Q(\sqrt{2\gamma}) = Q(\sqrt{2\lambda_o \gamma_c \gamma_L}) \quad (36)$$

$$\begin{aligned} I_{\mathbf{X},k}^{(2)} = & \sqrt{\frac{\lambda_k^{(\mathbf{X})} P_k^{(\mathbf{X})}}{\lambda_o P_o}} \frac{\alpha_{k,i,j}^{(\mathbf{X})} \beta_{o,s,v} c_k^{(\mathbf{X})}[j] c_o[v]}{T_o} \\ & \times \sum_{\ell=0}^{L-1} \int_{\ell T_k^{(\mathbf{X})}}^{(\ell+1)T_k^{(\mathbf{X})}} b_{k,i}^{(\mathbf{X})}(t - \tau_k^{(\mathbf{X})}) g_k^{(\mathbf{X})}(t - \tau_k^{(\mathbf{X})}) g_o(t) \cos(2\pi(f_{i,j} - f_{s,v})t + \theta_{k,i,j}^{(\mathbf{X})}) dt \\ = & \sqrt{\frac{\lambda_k^{(\mathbf{X})} P_k^{(\mathbf{X})}}{\lambda_o P_o}} \frac{\alpha_{k,i,j}^{(\mathbf{X})} \beta_{o,s,v} c_k^{(\mathbf{X})}[j] c_o[v]}{T_o} \sum_{\ell=0}^{L-1} \{ b_{k,i}^{(\mathbf{X})}[\ell-1] R_{\ell}(\tau_k^{(\mathbf{X})}, \theta_{k,i,j}^{(\mathbf{X})}) + b_{k,i}^{(\mathbf{X})}[\ell] \tilde{R}_{\ell}(\tau_k^{(\mathbf{X})}, \theta_{k,i,j}^{(\mathbf{X})}) \} \quad (23) \end{aligned}$$

$$R_{\ell}(\tau_k^{(\mathbf{X})}, \theta_{k,i,j}^{(\mathbf{X})}) = \int_{\ell T_k^{(\mathbf{X})}}^{\ell T_k^{(\mathbf{X})} + \tau_k^{(\mathbf{X})}} g_k^{(\mathbf{X})}(t - \tau_k^{(\mathbf{X})}) g_o(t) \cos(2\pi(f_{i,j} - f_{s,v})t + \theta_{k,i,j}^{(\mathbf{X})}) dt \quad (24)$$

$$\tilde{R}_{\ell}(\tau_k^{(\mathbf{X})}, \theta_{k,i,j}^{(\mathbf{X})}) = \int_{\ell T_k^{(\mathbf{X})} + \tau_k^{(\mathbf{X})}}^{(\ell+1)T_k^{(\mathbf{X})}} g_k^{(\mathbf{X})}(t - \tau_k^{(\mathbf{X})}) g_o(t) \cos(2\pi(f_{i,j} - f_{s,v})t + \theta_{k,i,j}^{(\mathbf{X})}) dt. \quad (25)$$

where $Q(x) = (1/\sqrt{2\pi}) \int_x^\infty e^{-t^2/2} dt$. Referring to [7], [15], and averaging (36) over the pdf of γ_L from (35), we can further simplify the conditional error probability for a given PCE λ_o as

$$\begin{aligned} P(e|\lambda_o) &= \int_0^\infty Q(\sqrt{2\lambda_o\gamma_c\gamma_L})f(\gamma_L)d\gamma_L \\ &= \left[\frac{1}{2} \left(1 - \sqrt{\frac{\lambda_o\gamma_c}{1+\lambda_o\gamma_c}} \right) \right]^M \\ &\quad \times \sum_{n=0}^{M-1} \binom{M-1+n}{n} \times \left[\frac{1}{2} \left(1 + \sqrt{\frac{\lambda_o\gamma_c}{1+\lambda_o\gamma_c}} \right) \right]^n. \end{aligned} \quad (37)$$

IV. EFFECT OF PCE ON BER PERFORMANCE

Now, we consider the effect of power control errors. According to [15] and [21], the open-loop PCE can be modeled as a log-normally distributed random variable with standard deviation σ_e in the decibels domain and mean $\bar{\lambda} = \exp\{(b\sigma_e)^2/2\}$, where $b = \ln 10/10$. Let $\delta = 10\log_{10}\lambda_o$. Then, δ becomes a normal distributed random variable with zero-mean and standard deviation σ_e . Averaging $P(e|\lambda_o)$ of (37) over the pdf of λ_o , we can obtain the total error probability $P(e)$ as in (38) shown at the bottom of the page, where

$$\mu(\delta) = \sqrt{\frac{10^{\delta/10}\gamma_c}{1+10^{\delta/10}\gamma_c}}. \quad (39)$$

Based on the Hermite polynomial approach of [22], the integration for a function $q(x)e^{-x^2}$ can be computed by

$$\int_{-\infty}^{\infty} q(x)e^{-x^2} dx = \sum_{i=1}^H \omega_i q(x_i) \quad (40)$$

where x_i and ω_i are the abscissas and the weight factor of the Hermite polynomials with order D , respectively. Letting $\delta = \sqrt{2}\sigma_e x$ in (38), we can further simplify the total error probability $P(e)$ to (41) shown at the bottom of the page. For the single-carrier DS-CDMA, the influence of the PCE was investigated by means of the first-order Taylor expansion method in [15]. However, this method is only suitable for a small PCE ($\sigma_e \leq 1$ dB) and small diversity order ($L \leq 3$). Our approach can evaluate the effect of a larger PCE (i.e., $\sigma_e \geq 1$ dB) and a higher diversity order for the multicarrier DS-CDMA system.

Unlike that the diversity order in the single-carrier DS-CDMA system means path diversity, the diversity order in the MC-DS-CDMA system means the frequency-domain diversity.

V. NUMERICAL RESULTS

In this section, we apply the developed analytical models to evaluate the joint impact of the complete MAI and the PCE on the error probability and capacity performances of a multirate MC-DS-CDMA system. In order to have the complete frequency diversity gain, the frequency separations for the M subcarriers carrying the same data bit follow the assumption of (6). We adopt the following parameters in most examples unless they are defined again.

- 1) The total number of subcarriers is 512 ($UM = 512$), where M is the frequency-domain spreading factor and U is the size of the serial-to-parallel process.
- 2) Variable data rates are achieved by changing the time-domain spreading factors in a set of $\{\max(G_o), \max(G_o)/2, \max(G_o)/4\}$ for a fixed frequency-domain spreading factor M .
- 3) There exist total 12 asynchronous users in the system, where three equal-numbered groups are formed. These three groups transmit data rates with frequency-domain and time-domain spreading factor $(M, \max(G_o))$, $(M, \max(G_o)/2)$, $(M, \max(G_o)/4)$, respectively.
- 4) The maximum total spreading gain is 256, i.e., $M \times \max(G_o) = 256$.
- 5) The Hermite polynomials order D used in (41) is 20.

A. Discussions

Here, we first qualitatively discuss the the error probability by observing the received signal-to-noise and interference ratio (SINR) γ defined in (31). For the sake of convenience, we assume that the bit energy (E_o) and the E_o/N_0 is large enough to ignore the influence of noise on the error probability. Note that $E_o = P_o T_o = P_k^{(X)} T_k^{(X)}$ (i.e., $P_k^{(X)} G_k^{(X)} = P_o G_o$ is fixed). Thus, we can rewrite (31) as

$$\gamma \approx \frac{(\frac{\lambda_o}{\lambda}) G_o \sum_{v=1}^M |\alpha_{o,s,v}|^2}{\sum_{\mathbf{X} \in \{A,B,C\}} \sum_{k=1}^{K_{\mathbf{X}}} 2 \frac{P_k^{(X)}}{P_o} \left(\frac{1}{3} + (UM-1)I_{oc} \right)}. \quad (42)$$

In this paper, variable data rates are achieved by changing the time-domain spreading factors in a set of

$$P(e) = \frac{1}{\sqrt{2\pi\sigma_e^2}} \int_{-\infty}^{\infty} \left[\frac{(1-\mu(\delta))}{2} \right]^M \sum_{n=0}^{M-1} \binom{M-1+n}{n} \left[\frac{(1+\mu(\delta))}{2} \right]^n e^{-\delta^2/2\sigma_e^2} d\delta \quad (38)$$

$$P(e) \approx \frac{1}{\sqrt{\pi}} \sum_{i=1}^D \omega_i \left[\frac{(1-\mu(\sqrt{2}\sigma_e x_i))}{2} \right]^M \sum_{n=0}^{M-1} \binom{M-1+n}{n} \left[\frac{(1+\mu(\sqrt{2}\sigma_e x_i))}{2} \right]^n \quad (41)$$

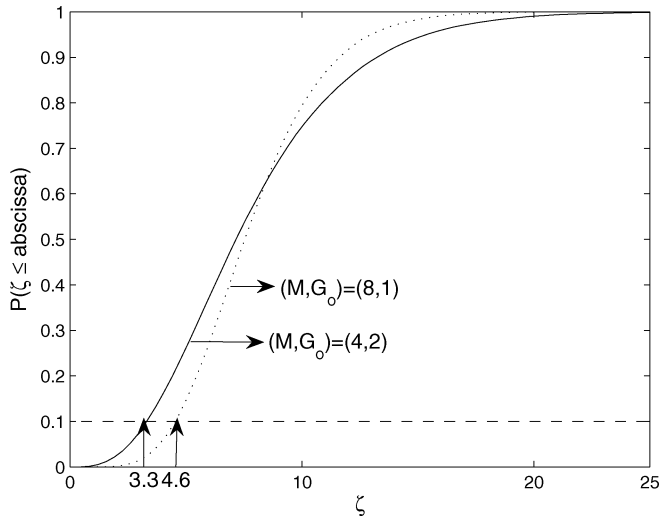


Fig. 4. Cumulative density functions of $\zeta = G_o \sum_{v=1}^M |\alpha_{o,s,v}|^2$ for $(M, G_o) = (4, 2)$ and $(M, G_o) = (8, 1)$.

$\{\max(G_o), \max(G_o)/2, \max(G_o)/4\}$ for a fixed frequency-domain spreading factor M . Therefore, the ratio of different transmission power is fixed for various values of G_o , i.e., $P_k^{(X)}/P_o$ is fixed. Note that $P_k^{(X)}/P_o = R_k^{(X)}/R_o$ [13], [20]. According to (42), we summarize the impacts of the power control error ($\lambda_o/\bar{\lambda}$), the transmission powers (P_o and $P_k^{(X)}$), the frequency-domain spreading gain (M), and the time-domain spreading gain (G_o) on the error probability in the following.

- 1) With fixed M and $\lambda_o/\bar{\lambda}$, a high data rate user can have better error rate performance because the high data rate user experience small amount of interference produced by low data rate users transmitting at lower power, i.e., $P_k^{(X)}$ is smaller.
- 2) With the same conditions as above, a larger time-domain spreading factor (G_o) can lead to a lower error probability because of the larger spreading gain.
- 3) With fixed G_o and $\lambda_o/\bar{\lambda}$, increasing the frequency-domain spreading gain (M) can result in a better error rate performance because of the larger frequency-diversity gain.
- 4) With fixed M , a larger G_o can make error probability more sensitive to power control errors because the larger G_o can magnify a minor change of $\lambda_o/\bar{\lambda}$. Thus, a better error rate performance thanks to a larger G_o comes at the cost of being more sensitive to power control errors.
- 5) Similar to the above phenomenon, a large M can also raise the sensitivity of the error probability to power control errors, although larger frequency-domain spreading gain can result in a lower error probability.
- 6) With a fixed product of $M \times G_o$, frequency-domain spreading (M) in the MC-DS-CDMA system is more sensitive to power control errors than time-domain spreading (G_o). To compare $(M, G_o) = (4, 2)$ and $(8, 1)$, we let $\zeta = G_o \sum_{v=1}^M |\alpha_{o,s,v}|^2$. Fig. 4 shows the cumulative density functions of ξ for $(M, G_o) = (4, 2)$ and $(8, 1)$. From the figure, one can find the 90th percentile of ξ for $(M, G_o) = (8, 1)$ is 4.6 which is larger than 3.3 for

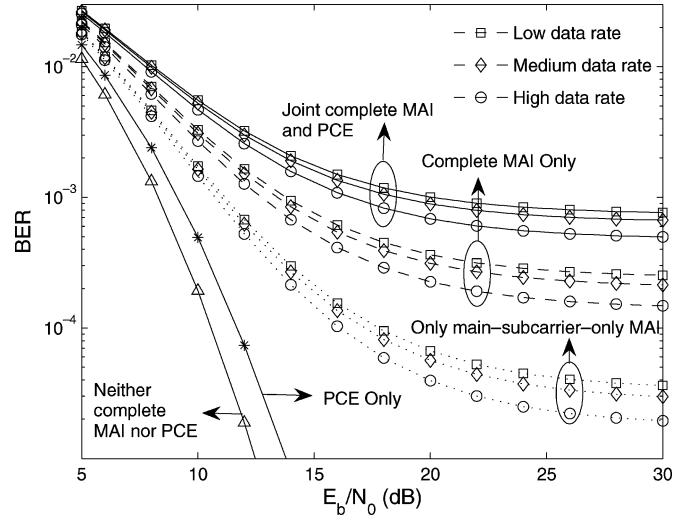


Fig. 5. The impact of the joint effect of complete MAI and PCE on the error rate performance of the MC-DS-CDMA system with $(M, G_o) = (8, 8)$, $(8, 16)$, and $(8, 32)$, where $M \times \max(G_o) = 256$ and the standard deviation of PCE $\sigma_e = 1.5$ dB.

$(M, G_o) = (4, 2)$. Thus, the case of $(M, G_o) = (8, 1)$ results in larger diversity gain than $(M, G_o) = (4, 2)$. That is, the case of $(M, G_o) = (8, 1)$ can amplify a small change of $\lambda_o/\bar{\lambda}$ more than the case of $(M, G_o) = (4, 2)$. Hence, $(M, G_o) = (8, 1)$ is also more sensitive to power control errors.

B. Impact of Complete MAI and PCE on Bit Error Probability

Fig. 5 shows the joint effect of complete MAI and PCE on the error rate performance of the MC-DS-CDMA system. Assume that 12 asynchronous users be equally partitioned into three groups with the frequency-domain and time-domain spreading factors $(M, G_o) = (8, 8)$, $(8, 16)$, and $(8, 32)$, respectively. First, without power control, we have following important observations.

- Compared with the effect of the main-subcarrier-only MAI, the complete MAI from all the intersubcarriers significantly degrades the BER performance. For $P(e) = 1.5 \times 10^{-3}$ and $(M, G_o) = (8, 8)$, the required E_b/N_0 is 10 dB in the main-subcarrier-only MAI case, while the required E_b/N_0 is increased to 12 dB in the complete MAI case.
- High data rate users have better BER performance compared with low data rate users. This observation confirms the first point of qualitative analysis in Section V.
- Note that both the main-subcarrier-only MAI and the complete MAI result in a floor of error probability in the region of high E_b/N_0 . In the former case, the error floor is about 1.95×10^{-5} , while in the latter case the error floor is increased to 1.47×10^{-4} .

Now, we consider the impact of PCE. In the figure, the standard deviation of PCE $\sigma_e = 1.5$ dB. For comparison, we also show the case with the single user and perfect power control (the curve with the legend “Neither complete MAI nor PCE”) and the case with the single user and imperfect power control (the curve with the legend “PCE only”). We observe that PCE exacerbates

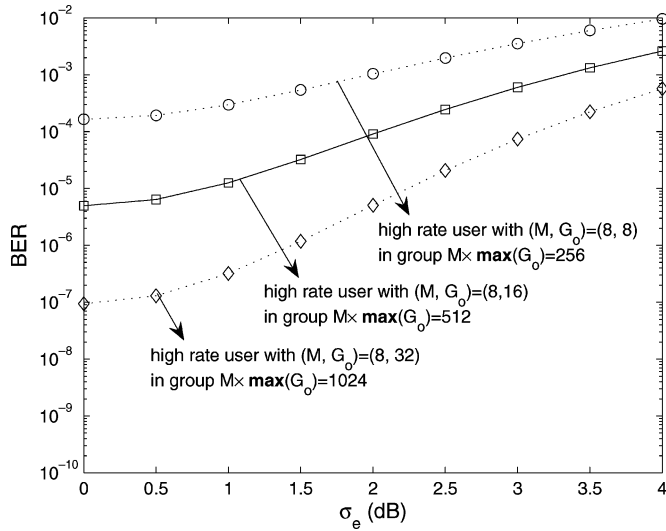


Fig. 6. The impact of PCE on the error rate performance of the MC-DS-CDMA system with a fixed frequency-domain spreading factors ($M = 8$) and various time-domain spreading factors $G_o = 8, 16$, and 32 for $M \times \max(G_o) = 256, 512$, and 1024 , respectively, when $E_b/N_0 = 25$ dB.

the effect of the complete MAI. That is, the increase of the required E_b/N_0 due to the joint PCE and complete MAI is indeed higher than the summation of those due to PCE only and complete MAI only individually. For $P(e) = 10^{-3}$, the required E_b/N_0 are 8.2, 9.1, 13.8, and 16.8 dB for the cases of “Neither complete MAI nor PCE,” “PCE only,” “Complete MAI only,” and “Joint complete MAI and PCE,” respectively. Compared with the based-line case of “Neither complete MAI nor PCE,” the effect of power control errors increases the required E_b/N_0 by 0.9 dB (i.e., the difference of 8.2 and 9.1 dB), while the effect of the complete MAI increases the required E_b/N_0 by 5.6 dB (i.e., the difference of 8.2–13.8 dB). However, the joint effect of the complete MAI and PCE increases the required E_b/N_0 by 8.6 dB (i.e., the difference of 16.8 and 8.2 dB). As a result, the joint effect of complete MAI and PCE further degrades the performance by 2.1 dB compared with the sum of the degradation from complete MAI only and PCE only individually.

C. Impact of Various Time-Domain and Frequency-Domain Spreading Factors

Fig. 6 shows the impact of various time-domain spreading factors and PCE on the multirate MC-DS-CDMA system when frequency-domain spreading factor $M = 8$ and $E_b/N_0 = 25$ dB. The error rate performances of three groups of spreading factors for $M \times \max(G_o) = 256, 512$, and 1024 are compared. To ease illustration, we only show the performances with the highest data rate in each group, i.e., $(8,8)$, $(8,16)$, and $(8,32)$. In general, we find that a larger maximum total spreading gain by increasing the time-domain spreading factor can improve the performance. This is mainly because users transmit lower power in a group of a larger maximum total spreading gain, thereby yielding fewer interference. Note that the product of the frequency-domain spreading gain and the time-domain spreading gain is not the only factor to determine the system performance. It is also influenced by various levels

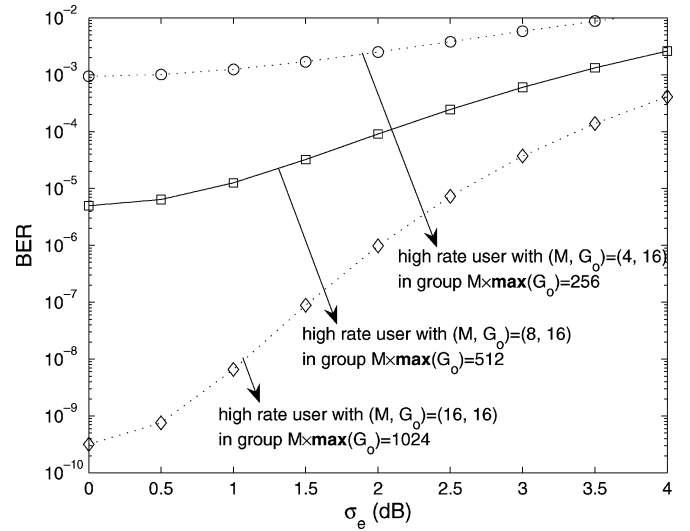


Fig. 7. The impact of PCE on the error rate performance of the MC-DS-CDMA system with a fixed time-domain spreading factors ($G_o = 16$) and various frequency-domain spreading factors $M = 4, 8$, and 16 for $M \times \max(G_o) = 256, 512$, and 1024 , respectively, when $E_b/N_0 = 25$ dB.

of transmission power from surrounding multirate users. In Fig. 6, the group with $M \times \max(G_o) = 256$ means that four users are allocated with the rates $(M, G_o) = (8, 8)$, $(8, 16)$, $(8, 32)$, respectively. Thus, the user with $(M, G_o) = (8, 32)$ in this group belongs to the low rate user and will experience the interference from three low-rate users with $(M, G_o) = (8, 32)$, four medium-rate users with $(M, G_o) = (8, 16)$, and four high rate user with $(M, G_o) = (8, 8)$. Similarly, a user with $(M, G_o) = (8, 32)$ in the group with $M \times \max(G_o) = 1024$ is classified to a high rate user, who will be interfered by three other high-rate users with $(M, G_o) = (8, 32)$, four medium-rate users with $(M, G_o) = (8, 64)$, and four low rate users with $(M, G_o) = (8, 128)$. Due to less interference, a user with $(M, G_o) = (8, 32)$ in the group of $M \times \max(G_o) = 1024$ indeed outperforms the user with $(M, G_o) = (8, 32)$ in the group of $M \times \max(G_o) = 256$. Our developed analytical model (i.e., (34)) can accurately calculate the MAI in the multirate MS-DS-CDMA system. Furthermore, due to the reason of the second point of the qualitatively analysis in Section V, the high rate user with $(M, G_o) = (8, 32)$ in the group of $M \times \max(G_o) = 1024$ can outperform the high rate user with $(M, G_o) = (8, 8)$ in the group of $M \times \max(G_o) = 256$, as shown in Fig. 5.

However, an MC-DS-CDMA system with a larger time-domain spreading factor also becomes more sensitive to PCE. When $(M, G_o) = (8, 8)$ and σ_e increasing from 0 to 4 dB, the error probability is increased by about an order of 10^2 (i.e., from 2.77×10^{-4} to 1.16×10^{-2}). For $(M, G_o) = (8, 32)$ in the same range of σ_e , the error probability is increased by about an order of 10^3 (i.e., from 1.88×10^{-7} to 7.49×10^{-4}). This phenomenon can be explained by the fourth point of the qualitative analysis in Section V. Thus, power control errors can reduce the performance benefits resulting from a larger time-domain spreading factor.

In Fig. 7, the impact of PCE on the multirate MC-DS-CDMA system is evaluated for a fixed time-domain spreading factor

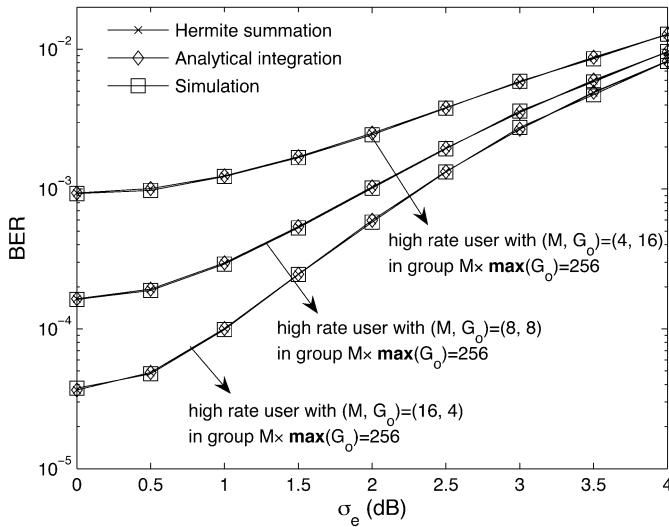


Fig. 8. The impact of PCE on the error rate performance of the MC-DS-CDMA system with various combinations of $(M, G_o) = (4, 16)$, $(8, 8)$, and $(16, 4)$, where $M \times \max(G_o) = 256$ and $E_b/N_0 = 25$ dB.

($G_o = 16$) and changing the frequency-domain spreading factors when $E_b/N_0 = 25$ dB. Consider three sets of spreading factors for $M \times \max(G_o) = 256, 512,$ and 1024 . Here, we only show the performance with $(M, G_o) = (4, 16)$ for $M \times \max(G_o) = 256, (8, 16)$ for $M \times \max(G_o) = 512,$ and $(16, 16)$ for $M \times \max(G_o) = 1024$. In the figure, as stated in the third and fifth points of the qualitative analysis in Section V, a larger maximum total spreading gain by increasing the frequency-domain spreading factor results in better performance due to a larger frequency-domain diversity gain but the sensitivity of the system to PCE also becomes higher. For example, when $M = 4$ and σ_e increases from 0 to 4 dB, the error probability changes from the order of 10^{-4} to 10^{-2} , whereas for $M = 16$ the error probability changes from the order of 10^{-10} to 10^{-4} . When the frequency-domain spreading factor (M) increases, the aggregated PCE's among M subcarriers become quite significant, and therefore reduce the advantage of frequency diversity over the system with a smaller frequency-domain spreading factor.

Interestingly, by comparing Figs. 6 and 7, one can find that frequency-domain spreading (M) in the MC-DS-CDMA system is more sensitive to power control errors than time-domain spreading (G_o). This phenomena can be explained by the sixth point of the qualitative analysis. To further confirm the above interesting observation, we perform simulations and evaluate the BER of MC-DS-CDMA systems according to (38) to illustrate the impact of PCE (σ_e) with various combinations of frequency-domain and time-domain spreading factors, as shown in Fig. 8. We let the maximum total spreading gain $M \times \max(G_o) = 256$ in this example. First, it is shown that the Hermite approach can accurately match both the analytical integration results and the simulation results. Second and more importantly, comparing the result of $(M, G_o) = (16, 4)$ with $(M, G_o) = (4, 16)$, we find that the performance improvement thanks to a larger frequency spreading factor is reduced as σ_e increases. For $\sigma_e = 0$ dB, changing the spreading factor from $(M, G_o) = (4, 16)$ to $(M, G_o) = (16, 4)$ can improve the bit error rate $P(e) = 9.3 \times 10^{-4}$ to $P(e) = 3.7 \times 10^{-5}$.

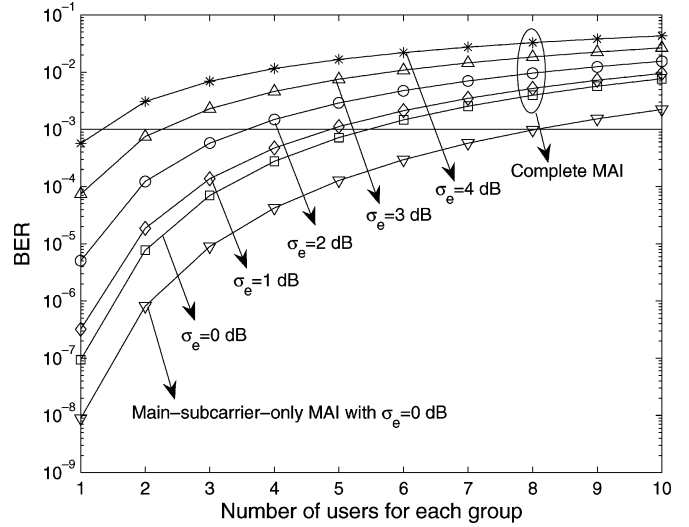


Fig. 9. The impact of complete MAI and PCE on the capacity of the multirate MC-DS-CDMA system with $\{(M, G_o)\} = \{(8, 8), (8, 16), (8, 32)\}$.

However, in the case of $\sigma_e = 4$ dB, $P(e) = 9.5 \times 10^{-3}$ for $(M, G_o) = (4, 16)$ and $P(e) = 8.2 \times 10^{-3}$ for $(M, G_o) = (16, 4)$. Although the system with a larger frequency-domain spreading factor still performs better than that with a smaller frequency spreading factor, the difference between the two becomes quite insignificant in the presence of a large power control error.

D. Impact of Complete MAI and PCE on Capacity

Fig. 9 shows the impact of the complete MAI and PCE on the capacity of the multirate MC-DS-CDMA system with time-domain and frequency-domain spreading factors in the group of $M \times \max(G_o) = 256, M = 8$ and $E_b/N_0 = 25$ dB. In the figure, the total number of users is three times the abscissa and the only the curve of $(M, G_o) = (8, 32)$ is drawn for each case. For a given $P(e) = 10^{-3}$ requirement and $\sigma_e = 0$ dB, the numbers of acceptable users in each group are eight and five for the main-subcarrier-only MAI and the complete MAI, respectively. The capacity decreases by 37.5%. However, for PCE $\sigma_e = 3$ dB and the complete MAI, is the number of acceptable users becomes two. That is, the joint effect of the PCE and the complete MAI can further decrease the capacity by 60% (from 5 to 2). Clearly, the effect of PCE worsens the impact of the complete MAI on the capacity of the multirate MC-DS-CDMA system. This phenomenon can be explained by observing the parameter $\bar{\lambda}$ (denoting the average power control error) in γ_c of (33), where the joint effect of PCE and complete MAI is analytically modeled by the term $\sum_{\mathbf{X} \in \{A, B, C\}} \sum_{k=1}^{K_{\mathbf{X}}} [2\bar{\lambda} P_k^{(\mathbf{X})} (1/3 + (UM - 1)I_{oc})] / (P_o G_o)$.

VI. CONCLUDING REMARKS

In this paper, we have developed an analytical model to quantitatively evaluate the performance of multirate MC-DS-CDMA systems using time- and frequency-domain spreading codes subject to the PCE and the complete MAI from all subcarriers. Applying the developed analytical model, we have obtained the following observations.

- When both PCE and the complete MAI are jointly considered, the effect of PCE can exacerbate the impact of complete MAI on the MC-DS-CDMA system, or *vice versa*.
- A larger maximum total spreading gain either by increasing frequency- or time-domain spreading factors can enhance the performance of the multirate MC-DS-CDMA system. However, the sensitivity of these performance gains to power control errors cannot be ignored.
- A larger PCE (σ_e) can possibly make the frequency-domain diversity gain diminish faster than the gain obtained from the time-domain spreading. Thus, although for the same maximum total time and frequency spreading gain, the MC-DS-CDMA system with a larger frequency-domain spreading factor results in better performance than that with a larger time-domain spreading factor, the performance difference between the two become less significant as power control errors increase.

The developed analytical model and the above observations can provide some important insights into the performance issues of multirate MC-DS-CDMA systems. Possible interesting research topics that can be extended from this work include: 1) to analyze the multirate MC-DS-CDMA system under other types of fading channels [12], [23] and other distortion [24] subject to power control errors and complete MAI and 2) to develop resource allocation mechanisms including code assignment, subcarrier allocation [25], scheduling [26], and power control schemes [27] for the multirate MC-DS-CDMA system.

APPENDIX I

In this appendix, we derive $\text{Var}[R(\tau_k^{(\mathbf{X})}, \theta_{k,i,j}^{(\mathbf{X})})]$. To ease the notation, let $\tau_k^{(\mathbf{X})} = \tau$ and $\theta_{k,i,j}^{(\mathbf{X})} = \theta$. Then, we can calculate $\text{Var}[R(\tau_k^{(\mathbf{X})}, \theta_{k,i,j}^{(\mathbf{X})})]$ by

$$\text{Var}[R(\tau, \theta)] = E_\tau[E_\theta[R^2(\tau, \theta)]] \quad (43)$$

Recall that in the case of ($0 \leq \tau_k^{(\mathbf{X})} < T_o$), τ is uniformly distributed in $[0, T_o)$. Hence, we assume that $hT_c \leq \tau < (h+1)T_c$, where $0 \leq h \leq G_o - 1$ and G_o is the time-

main spreading factor of the reference user. Following the same procedure as [7], we have (44) shown at the bottom of the page. Then, the expectation of (44) with respect to τ over $[0, T_o)$ can be obtained by calculating (45)–(46) shown at the bottom of the page. Similarly, we can obtain

$$\begin{aligned} \text{Var}[\tilde{R}(\tau, \theta)] &= \text{Var}[R(\tau, \theta)] \quad (47) \\ &= \frac{G_o T_c^2}{4\pi^2[(i-s) + (j-v)U]^2}. \quad (48) \end{aligned}$$

APPENDIX II

Here, we derive $\text{Var}[R(T_o, \theta_{k,i,j}^{(\mathbf{X})})]$. Let $\tau_k^{(\mathbf{X})} = \tau$ and $\theta_{k,i,j}^{(\mathbf{X})} = \theta$ without loss of generality. Then, $\text{Var}[R(T_o, \theta_{k,i,j}^{(\mathbf{X})})]$ can be calculated as

$$\text{Var}[R(T_o, \theta)] = E_\tau[E_\theta[R^2(T_o, \theta)]] \quad (49)$$

Recall that τ and θ are uniformly distributed in $[T_o, T_k^{(\mathbf{X})})$ and $[0, 2\pi)$, respectively. Assume $hT_c \leq \tau < (h+1)T_c$, where $G_o \leq h \leq G_k^{(\mathbf{X})} - 1$; G_o and $G_k^{(\mathbf{X})}$ are the time-domain spreading factors of the reference user and the interfering user, respectively. Then, referring to (10), we can express $R(T_o, \theta)$ as

$$\begin{aligned} R(T_o, \theta) &= \sum_{j=0}^{G_o-1} g_o[j] g_k^{(\mathbf{X})} [G_k^{(\mathbf{X})} - h - 1 + j] \\ &\quad \times \int_{jT_c}^{jT_c + \tau - hT_c} \cos\left(\frac{2\pi z t}{T_c} + \theta\right) dt \\ &\quad + \sum_{j=0}^{G_o-1} g_o[j] \times g_k^{(\mathbf{X})} [G_k^{(\mathbf{X})} - h + j] \\ &\quad \times \int_{jT_c + \tau - hT_c}^{(j+1)T_c} \cos\left(\frac{2\pi z t}{T_c} + \theta\right) dt \quad (50) \end{aligned}$$

where

$$z = (i-s) + (j-v)U \quad (51)$$

$$\begin{aligned} E_\theta[R^2(\tau, \theta)] &= \frac{1}{2} \int_{hT_c}^{(h+1)T_c} \left\{ (\tau - hT_c)^2 \times \text{sinc}^2\left(\frac{\pi z(\tau - hT_c)}{T_c}\right) (h+1) + ((h+1)T_c - \tau)^2 \times \text{sinc}^2\left(\frac{\pi z((h+1)T_c - \tau)}{T_c}\right) h \right\} d\tau \quad (44) \end{aligned}$$

$$\begin{aligned} \text{Var}[R(\tau, \theta)] &= \frac{1}{2T_o} \sum_{h=0}^{G_o-1} \int_{hT_c}^{(h+1)T_c} \left\{ (\tau - hT_c)^2 \times \text{sinc}^2\left(\frac{\pi z(\tau - hT_c)}{T_c}\right) (h+1) + ((h+1)T_c - \tau)^2 \times \text{sinc}^2\left(\frac{\pi z((h+1)T_c - \tau)}{T_c}\right) h \right\} d\tau \quad (45) \end{aligned}$$

$$= \frac{G_o T_c^2}{4\pi^2[(i-s) + (j-v)U]^2} \quad (46)$$

$$\begin{aligned} \text{Var}[R(T_o, \theta)] &= \frac{G_o}{2(T_k^{(X)} - T_o)} \sum_{h=G_o}^{G_k^{(X)}-1} \int_{hT_c}^{(h+1)T_c} (\tau - hT_c)^2 \times \text{sinc}^2\left(\frac{\pi z}{T_c}(\tau - hT_c)\right) + [(h+1)T_c - \tau]^2 \times \text{sinc}^2\left(\frac{\pi z}{T_c}((h+1)T_c - \tau)\right) d\tau \quad (56) \\ &= \frac{G_o T_c^2}{2\pi^2[(i-s) + (j-v)U]^2} \end{aligned} \quad (57)$$

After some deductions, we obtain

$$\begin{aligned} R(T_o, \theta) &= (\tau - hT_c) \text{sinc}\left(\frac{\pi z}{T_c}(\tau - hT_c)\right) \\ &\quad \times \sum_{j=0}^{G_o-1} g_o[j] \times g_k^{(X)}[G_k^{(X)} - h - 1 + j] \cos\Phi_{j,\tau}^{(1)} \\ &\quad + [(h+1)T_c - \tau] \times \text{sinc}\left(\frac{\pi z}{T_c}((h+1)T_c - \tau)\right) \\ &\quad \times \sum_{j=0}^{G_o-1} g_o[j] g_k^{(X)}[G_k^{(X)} - h + j] \cos\Phi_{j,\tau}^{(2)} \quad (52) \end{aligned}$$

where

$$\Phi_{j,\tau}^{(1)} = \frac{\pi z}{T_c}(2jT_c + \tau - hT_c) + \theta \quad (53)$$

$$\Phi_{j,\tau}^{(2)} = \frac{\pi z}{T_c}((2j+1)T_c + \tau - hT_c) + \theta. \quad (54)$$

Taking the expectation of $R^2(T_o, \theta)$ respective to θ over $[0, 2\pi)$, $g_o[j]$, and $g_k^{(X)}[j]$, where $g_o[j]$ and $g_k^{(X)}[j]$ are assumed to be ± 1 with equal probability, we can have

$$\begin{aligned} E_\theta[R^2(T_o, \theta)] &= \frac{G_o}{2} \left[(\tau - hT_c)^2 \text{sinc}^2\left(\frac{\pi z}{T_c}(\tau - hT_c)\right) \right. \\ &\quad \left. + [(h+1)T_c - \tau]^2 \text{sinc}^2\left(\frac{\pi z}{T_c}((h+1)T_c - \tau)\right) \right]. \quad (55) \end{aligned}$$

Finally, substituting (55) into (49), we can get $\text{Var}[R(T_o, \theta)]$ by calculating (56)–(57) shown at the top of the page.

REFERENCES

- [1] D. K. Kim and S.-H. Hwang, "Capacity analysis of an uplink synchronized multicarrier DS-CDMA system," *IEEE Commun. Lett.*, vol. 6, pp. 99–101, Mar. 2002.
- [2] J. Namgoong, T. Wong, and J. Lehnert, "Subspace multiuser detection for multicarrier DS-CDMA," *IEEE Trans. Commun.*, vol. 48, no. 11, pp. 1897–1908, Nov. 2000.
- [3] S. Hara and R. Prasad, "Overview of multicarrier CDMA," *IEEE Commun. Mag.*, vol. 35, no. 12, pp. 126–133, Dec. 1997.
- [4] L. Loyola and T. Miki, "A new transmission and multiple access scheme based on multicarrier CDMA for future highly mobile networks," in *Proc. IEEE Int. Symp. Pers., Indoor and Mobile Radio Commun.*, vol. 2, Sep. 2003, pp. 1944–1948.
- [5] L.-L. Yang and L. Hanzo, "Multicarrier DS-CDMA: A multiple access scheme for ubiquitous broadband wireless communications," *IEEE Commun. Mag.*, vol. 41, no. 10, pp. 116–124, Oct. 2003.
- [6] D. K. Kim and S.-H. Hwang, "Capacity analysis of an uplink synchronized multicarrier DS-CDMA system," *IEEE Commun. Lett.*, vol. 6, pp. 99–101, Mar. 2002.
- [7] L. Hanzo, L.-L. Yang, E.-L. Kuan, and K. Yen, *Single and Multi-Carrier DS-CDMA Multi-User Detection, Space-Time Spreading, Synchronization, Networking and Standards*, 1st ed. New York: Wiley, 2003.
- [8] L.-L. Yang and L. Hanzo, "Generalized multicarrier DS-CDMA using various chip waveforms," in *Proc. IEEE Wireless Commun. Netw. Conf.*, vol. 51, May 2003, pp. 748–752.
- [9] —, "Performance of broadband multicarrier DS-CDMA using space-time spreading-assisted transmit diversity," *IEEE Trans. Wireless Commun.*, vol. 4, no. 3, pp. 885–894, May 2005.
- [10] J.-H. Rhee, M.-Y. Woo, and D.-K. Kim, "Multichannel joint detection of multicarrier 16-QAM DS/CDMA system for high-speed data transmission," *IEEE Trans. Veh. Technol.*, vol. 52, no. 1, pp. 37–47, Jan. 2003.
- [11] C. W. You and D. S. Hong, "Multicarrier CDMA systems using time-domain and frequency-domain spreading codes," *IEEE Trans. Commun.*, vol. 51, no. 1, pp. 17–21, Jan. 2003.
- [12] L.-L. Yang and L. Hanzo, "Performance of generalized multicarrier DS-CDMA over Nagagami- m fading channels," *IEEE Trans. Commun.*, vol. 50, no. 6, pp. 956–966, Jun. 2002.
- [13] K. S. Lim and J. H. Lee, "Performance of multirate transmission schemes for a multicarrier DS/CDMA system," in *Proc. IEEE Veh. Technol. Conf.*, vol. 2, Oct. 2001, pp. 767–771.
- [14] S. Ulukus and R. D. Yates, "Stochastic power control for cellular radio systems," *IEEE Trans. Commun.*, vol. 46, no. 6, pp. 784–798, Jun. 1998.
- [15] N. Kong and L. B. Milstein, "Error probability of multicell CDMA over frequency selective fading channels with power control error," *IEEE Trans. Commun.*, vol. 47, no. 4, pp. 608–617, Apr. 1999.
- [16] J. M. Romero-Jerez, M. Ruiz-Garcia, and A. Diaz-Estrella, "Effects of multipath fading on BER statistics in cellular CDMA networks with fast power control," *IEEE Commun. Lett.*, vol. 4, pp. 349–351, Nov. 2000.
- [17] Abrardo and D. Sennati, "On the analytical evaluation of closed-loop power-control error statistics in DS-CDMA cellular systems," *IEEE Trans. Veh. Technol.*, vol. 49, no. 6, pp. 2071–2080, Nov. 2000.
- [18] L.-C. Wang and C.-W. Chang, "Probability of false power control command in CDMA systems subject to measurement errors," *IEEE Commun. Lett.*, vol. 9, pp. 298–300, Apr. 2005.
- [19] M. Fisz, *Probability Theory and Mathematical Statistics*, 1st ed. New York: Krieger, 1963.
- [20] T. Ottosson and A. Svensson, "On schemes for multirate support in DS-CDMA systems," *Wireless Pers. Commun.*, vol. 6, no. 3, pp. 265–287, Mar. 1998.
- [21] H.-J. Su and E. Geraniotis, "Adaptive closed-loop power control with quantized feedback and loop filtering," *IEEE Trans. Wireless Commun.*, vol. 1, no. 1, pp. 76–86, Jan. 2002.
- [22] M. Abramowitz and I. A. Stegun, *Handbook of Mathematical Functions with Formulas, Graphs, and Mathematical Tables*: U.S. Dept. Commerce National Bureau of Standards, 1964, vol. 55, Applied Mathematics Series.
- [23] S. Hara and R. Prasad, "Design and performance of multicarrier CDMA system in frequency-selective Rayleigh fading channels," *IEEE Trans. Veh. Technol.*, vol. 48, no. 5, pp. 1584–1595, Sep. 1999.
- [24] L. Rugini and P. Banelli, "BER of MC-DS-CDMA systems with CFO and nonlinear distortions," in *Proc. IEEE Int. Conf. Acoustics, Speech, and Signal Processing*, vol. 4, May 2004, pp. iv773–iv776.
- [25] L. Hai and Y. H. Chew, "An adaptive subcarrier allocation scheme for MC-DS-CDMA systems in the presence of multiple access interference," in *Proc. IEEE Int. Conf. Commun.*, Jun. 2004, pp. 2894–2898.
- [26] H. Kim and Y. Han, "A proportional fair scheduling for multicarrier transmission systems," *IEEE Commun. Lett.*, vol. 9, pp. 210–212, Mar. 2005.
- [27] M. Hamza, H. T. Huynh, and P. Fortier, "Fixed and multiple step power control for MC-DS-CDMA in indoor and outdoor environments," in *Proc. IEEE Int. Conf. Commun.*, Jun. 2004, pp. 2965–2969.



Li-Chun Wang (M'96–SM'05) received the B.S. degree from the National Chiao Tung University, Hsinchu, Taiwan, R.O.C., in 1986, the M.S. degree from National Taiwan University, Taipei, Taiwan, R.O.C., in 1988, and the M.Sci. and Ph.D. degrees from the Georgia Institute of Technology, Atlanta, in 1995, and 1996, respectively, all in electrical engineering.

From 1990 to 1992, he was with the Telecommunications Laboratories, Ministry of Transportations and Communications, Taiwan (currently the Telecom Laboratories of Chunghwa Telecom Company). In 1995, he was affiliated with Bell Northern Research of Northern Telecom, Inc., Richardson, TX. From 1996 to 2000, he was with AT&T Laboratories, where he was a Senior Technical Staff Member in the Wireless Communications Research Department. Since August 2000, he has been an Associate Professor in the Department of Communication Engineering, National Chiao Tung University. He holds a U.S. patent and three more pending. His current research interests are in the areas of cellular architectures, radio network resource management, cross-layer optimization, and cooperation wireless communications networks.

Dr. Wang was a corecipient of the 1997 IEEE Jack Neubauer Best Paper Award for his paper "Architecture Design, Frequency Planning, and Performance Analysis for a Microcell/Macrocell Overlaying System," with G. L. Stuer and C.-T. Lea, in the IEEE TRANSACTIONS ON VEHICULAR TECHNOLOGY (best systems paper published in 1997 by the IEEE Vehicular Technology Society). Currently, he is serving as an Associate Editor for the IEEE JOURNAL ON SELECTED AREAS IN COMMUNICATIONS: Wireless Communications Series.



Chih-Wen Chang (S'02) received the B.S. and M.S. degrees in electrical engineering from the National Sun Yat-Sen University, Kaohsiung, Taiwan, R.O.C., in 1998 and 2000, respectively, the Minor M.S. degree in applied mathematics and the Ph.D. degree in communication engineering from the National Chiao-Tung University, Hsinchu, Taiwan, in 2005 and 2006, respectively.

His current research interests include wireless communications, wireless networks, and cross-layer design.

Dr. Chang was awarded the IEEE Student Travel Grant for ICC 2006.